Journal of Electronic Materials (2022) 51:4790–4801
https://doi.org/10.1007/s11664-022-09746-w

TOPICAL COLLECTION: SYNTHESIS AND ADVANCED CHARACTERIZATION OF MAGNETIC OXIDES

High Strain Response and Dielectric Properties of $Bi_{1/2}(Na_{0.78}K_{0.22})_{1/2}TiO_3$ Ceramics Doped with $(Fe_{1/2}Nb_{1/2})^{4+}$

Saima Naz[1] · Amir Ullah[1] · Aurang Zeb[1] · Fazli Akram[2] · Abdennaceur Karoui[2] · Muhammad Sheeraz[3] · Chang Won Ahn[3]

Received: 7 November 2021 / Accepted: 1 June 2022 / Published online: 23 June 2022

Abstract

Environmentally friendly piezoceramics $Bi_{1/2}(Na_{0.78}K_{0.22})_{1/2}Ti_{1-x}(Fe_{1/2}Nb_{1/2})_xO_3$ (BNKT-FN) with FeNb (FN) ratios 0, 0.01, 0.02, 0.03 and 0.04 were synthesized via conventional solid-state reaction (CSSR). X-ray diffraction (XRD) analysis revealed that the FN complexes were completely dissolved in BNKT perovskite and the structural transition occurred from ferroelectric to relaxor state. The average grain sizes for $x=0$, 0.01, 0.02, 0.03 and 0.04 were found to be 0.34 μm, 0.35 μm, 0.38 μm, 0.32 μm and 0.39 μm, respectively. It is observed that the grain size increased with the addition of FN, except for $x=0.03$. The coercive field (E_c) and remnant polarization (P_r) of the system were decreased with increasing FN concentration and the highest E_c of 21.1 kV/cm and P_r of 29.2 μC/cm^2 were noted for the base pure sample. In addition, the increase of FN content steadily broadened the dielectric anomaly at maximum dielectric constant temperature (T_m) in the BNKT-FN system. Consequently, unipolar normalized strain (S_{max}/E_{max}) was found to be enhanced monotonically achieving the highest value of around 654 pm/V ($x=0.02$). These properties suggest that the investigated system could be a promising eco-friendly candidate for piezoelectric actuators and many other applications requiring high piezoelectric induced strain.

Keywords Lead-free · high piezoelectric strain · BNKT-based ceramics · complex ion doping · ferroelectrics · dielectrics

Introduction

For the electromechanical actuator, the essential property is the electric field-induced strain (EFIS) in the piezoelectric materials. Lead zirconate titanate $Pb(Zr,Ti)O_3$ (PZT) is the main piezoelectric material widely used for piezoelectric actuators, sensors, and transducers. Pb-based relaxor ferroelectrics, such as $Pb(Mg_{1/3}Nb_{2/3})O_3$-$PbTiO_3$ (PMN-PT) and $Pb_{1-x}La_x(Zr_{1-y}T_y)_{1-x/4}O_3$ (PLZT) systems show a high electromechanical strain and are widely used in actuator applications.[1–4] Nonetheless, due to environmental concerns about lead oxide toxicity, scientists/researchers have placed a strong emphasis on eco-friendly functional ceramics with a high strain response. Eco-friendly $Bi_{1/2}Na_{1/2}TiO_3$ (BNT)-based piezoelectric ceramics are suggested to be a favorable Pb-free material on account of their high electric field-induced strain (EFIS) level.[5–8] BNT is a perovskite and has remnant polarization, $P_r=38$ μC/cm^2 with a large coercive field of $E_c=73$ kV/cm. BNT has a rhombohedral structure, excellent dielectric properties and a high Curie temperature ($T_c\sim320$°C). But the disadvantage of BNT is its large coercivity ($E_c=73$ kV/cm), because of which its electric poling is quite difficult.[9,10] Therefore, BNT was deemed unsuitable for practical use in devices in the first place. Consequently, it was substitued with other perovskites such as $Bi_{1/2}K_{1/2}TiO_3$ (BKT). Furthermore, the BNT and BKT alloying, making $(1-x)$BNT-xBKT binary systems, display a morphotropic phase boundary (MPB) in the range $0.16\le x\le0.20$ and results in enhanced piezoelectric and ferroelectric characteristics compared with other Pb-free materials. The partial

✉ Amir Ullah
amirullah@icp.edu.pk

[1] Department of Physics, Islamia College, Peshawar, KP 25120, Pakistan

[2] Department of Mathematics and Physics/CREST Center, North Carolina Central University, Durham, NC 27707, USA

[3] Department of Physics and Energy Harvest Storage Research Center (EHSRC), University of Ulsan, Ulsan 44610, Republic of Korea

substitution of Na^+ by K^+ results in high EFIS response and excellent ferroelectric properties.[7,8]

BNKT was further doped with a single element on the *A*-site and/or *B*-site (*cations*) by, for instance, La_2O_3, Nb_2O_5, and by perovskites, such as $BaTiO_3$, for the purpose of decreasing the coercivity and enhancing the strain properties.[11–13] Pham et al.[5] studied the effect of Nb on $Bi_{1/2}(Na_{0.82}K_{0.18})_{1/2}TiO_3$ system and obtained a remarkable strain value of 0.47% with a Nb ratio of 3.0 mol.%. Ta-doped BNT-BKT ceramic alloys were also investigated and found to have a high strain.[14] The addition of these new additives is expected to have an impact on the EFIS and piezoelectric behavior of Pb-free BNT-based ceramics. Electromechanical strain is one of the core parameters for piezoelectric devices such as actuators and sensors.[15,16] Thus, BNT-based systems can be projected to perform as potential eco-friendly piezoelectric materials.

The displacement of *B*-site cations and oxygen anions causes polarization in a perovskite ferroelectric.[17–20] The replacement of *B*-site cations can reduce the ferroelectric behavior of ceramics, modify the nano-domain size, and further affect the strain response.[11–14,20] Scientists have focused on the replacement of cations at the *B*-site of BNT-based ceramics in order to get high strain by the disruption of the long-range dipole structure,[21–23] which significantly changes the electric balance.

Recently, researchers focused on a new approach (i.e introducing complex ion doping of the material) to study the influence of complex cations on strain properties in BNT-based lead-free materials. For instance, the influence of the chemically complex cations $(Fe_{1/2}Me_{1/2})^{4+}$ (Me = Sb, Nb and Ta) on the strain of 0.99 $Bi_{1/2}(Na_{0.8}K_{0.2})_{1/2}TiO_3$-0.01 $SrTiO_3$ system was studied by Liu et al.[24]. In another report, Li et al.,[25] studied the replacement of complex cations $(Al_{1/2}Sb_{1/2})^{4+}$ of 0.935 BNT-0.065 $BaTiO_3$ at the *B*-site and observed a large value of strain (0.46%) at an applied field of 80 kV/cm. Complex cations can effectively increase the *B*-site compositional disorder and disrupt the long range ferroelectric pattern. The very high strain value of 602 pm/V was obtained in $(Fe_{1/2}Nb_{1/2})$ doped BNBT ceramics, due to the $(Fe_{1/2}Nb_{1/2})^{4+}$ complex ion substitution of titanium (Ti^{4+}) at the B-site in $(Fe_{1/2}Nb_{1/2})$ doped $(Bi_{1/2}Na_{1/2})_{0.935}Ba_{0.065}TiO_3$ ceramics.[26]

Moreover, because combined Fe^{3+} (0.645 Å and CN = 6) and Nb^{5+} (0.60 Å and CN = 6) have nearly the same ionic size of Ti^{4+} (0.605 Å and CN = 6), the $(Fe_{1/2}Nb_{1/2})^{4+}$ complex ion will occupy the *B*-site and replace Ti^{4+} in the perovskite.[26] Accordingly, incorporation of $(Fe_{1/2}Nb_{1/2})^{4+}$ can distort the crystal lattice, and consequently, a high strain may be obtained in the BNT–BKT ceramics. Therefore, disturbance of the long ferroelectric pattern, as well as an increase in the strain, is likely. Given the significance of the complex ion, we proposed to use it as dopant for the BNKT system. $Bi_{1/2}(Na_{0.78}K_{0.22})_{1/2}TiO_3$ was chosen as the base composition because it has a tetragonal structure close to MPB of BNT–BKT and a high dynamic piezoelectric strain response ($d_{33}^* \approx 291$ pm/V).[8]

Therefore, $Fe_{1/2}Nb_{1/2}$ (FN) was used as a dopant for the planned system $Bi_{1/2}(Na_{0.78}K_{0.22})_{1/2}Ti_{1-x}(Fe_{1/2}Nb_{1/2})_xO_3$ (BNKT-FN) ($x = 0, 0.01, 0.02, 0.03, 0.04$) and the influence of FN ion on the structure, and the electrical and piezoelectric response were examined in detail. Note that FN sits the in *B*-site of BNKT. The rationale of the current studies is two-pronged: (i) fabrication and sintering of BNKT-FN ceramics by conventional solid-state reaction (CSSR) and (ii) their electrical characterization to unravel their piezoelectric, ferroelectric, and dielectric properties.

Experimental

Piezoelectric BNKT-FN ceramics were synthesized by CSSR for all above indicated stoichiometric ratios ($x = 0$, 0.01, 0.02, 0.03, 0.04). The raw materials in preparation included Na_2CO_3, Bi_2O_3, TiO_2, and K_2CO_3 (99.90% High Purity Chemicals, Japan), Fe_2O_3, and Nb_2O_5 (99.9% Cerac Specialty Inorganics, USA). To remove moisture, ceramics were dried at 100°C for 24 h followed by weighing the starting raw materials for the considered stoichiometric ratios. First, ball milling was carried out in bottles containing zirconia balls and ethanol for 12 h. The samples were again dried at 100°C for 24 h and then ground to a very fine size. Calcination was done at a temperature of 850°C for a duration of 2 h. Grinding of ceramics was again performed followed by second ball milling and drying at the same conditions as mentioned above. After grinding, powders were crushed and mixed with PVA (polyvinyl alcohol) solvent and then compacted at an optimum pressure of 100 MPa into disk-shaped pellets with a diameter of ≈ 10 mm. The pellets are densified at 1150°C for 2 h in crucibles. X-ray diffraction (XRD) of polished disks was done using a Rigaku XRD system model RAD III, with a step size of 0.02°. Monochromatic line CuK_α ($\lambda_{k\alpha} = 1.54178$ Å) was utilized.

Microstructural exploration was performed using a field-emission scanning electron microscope (FE-SEM) Hitachi S-4200. The 1-mm-thick pellets were polished to enable measurement of electrical properties. Electrodes on both disk surfaces were printed using silver paste through a screen and annealed at 700°C for 30 min. Temperature-dependent dielectric properties were obtained at temperatures ranging from room temperature to 500°C with a heating rate of 5°C/min by using an HP4192A impedance analyzer. The polarization hysteresis loops P-E were obtained at a frequency of 2 Hz at room temperature using a Sawyer–Tower circuit which applied an electric field of AC waveform. The electromechanical measurement was done at a frequency of

200 mHz by an in-house linear variable differential transducer (LVDT) of model MCH-331 & M401 by Mitutoyo Co.

Results and Discussion

Phase Assemblage and Bulk Microstructural Analysis

To find the phase structure of the synthesized BNKT-FN ceramics, an X-ray diffraction (XRD) study was performed in the 2θ range from 20° to 60° as depicted in Fig. 1a. Pure perovskite phase was obtained with no unwanted secondary phase for the system being investigated. Moreover, the incorporation of the FN amount affected the phase structure of the BNKT compound. Undoped BNKT-FN ceramics have a tetragonal structure, shown by the two split peak (002)/(200) at a 2θ of nearly 46.5° which is also evident from the (010)/(100) peak splitting at $2\theta \sim 22°$.[6,10] However, with the addition of FN, the intensity of the (002) peak gradually weakened. The decrease of (002) peak intensity was observed with increasing FN concentration. The variation of lattice parameters with FN concentration is shown in Fig. 1b. Lattice constant ***a*** is increased, and lattice constant ***c*** is decreased with increasing of x, while the ***c/a*** ratio is decreased, which may suggest a tetragonal (ferroelectric) to pseudocubic (relaxor) phase transformation as usually noticed in BNKT-based ceramics. The crystal structure as observed in the XRD was further confirmed by full pattern refinement as shown in Fig. 1c. For samples $x=0$ and 0.02, the data could be indexed to the two-phase tetragonal and cubic mixture ($P4mm + Pm\bar{3}m$). However, a single cubic phase with space group $Pm\bar{3}m$ was detected for sample $x=0.04$. Therefore, it was confirmed that the structure transformed from a mixed tetragonal-cubic phase to a single cubic phase when the FN amount was increased to $x=0.04$. All the samples showed the best fitting with an excellent goodness-of-fit factor ($\chi^2 \leq 3.83$).

Structural modifications of this type were also found with the partial Nb replacement of the *B*-site in the BNKT-based compound.[11] Doping BNKT ceramics with Fe resulted in enhancement of static piezoelectric coefficient (d_{33}) from 125 pC/N to 148 pC/N, and the depolarization temperature (T_d) was also increased from 76°C to 118°C.[27]

FE-SEM images and histogram of the deduced grain size distribution of BNKT-FN piezoelectric material with ratios $x=0$, 0.02, 0.03, and 0.04, sintered at 1150°C for 2 h are displayed in Fig. 2. It can be seen that all samples have dense microstructures with a few visible pores, while grains appear with clear grain boundaries. The micrograph of pure BNKT-FN ceramics comprises cubic and round-shaped grains. The grain morphology changes to a more regular round shape as the FN ratio increases. The average grain sizes for $x=0$, 0.01, 0.02, 0.03 and 0.04 were found to be 0.34 μm, 0.35 μm, 0.38 μm, 0.32 μm and 0.39 μm, respectively, which indicates a grain size increase with the FN content, except for $x=0.03$. The incorporation of low melting point FN components may increase the speed of ion diffusion, which resulted in grain size increase. Another reason may be because the ionic size of combined Fe^{3+} (0.645 Å) and Nb^{5+} (0.60 Å) is nearly the same as that of Ti^{4+} (0.605 Å); thus, the $(Fe_{1/2}Nb_{1/2})^{4+}$ complexion will occupy the *B*-site and replace Ti^{4+} in the perovskite.[26] Then, titanium and oxygen vacancies will be created. The oxygen and *B*-site vacancies in the oxide compound are helpful for mass transport during sintering.[26] The variation of the average grain size is listed in Table I.

Electrical Characterization

Dielectric Response

Figure 3 displays the relative permittivity ε_r) versus temperature (ε_r-T) and tangent loss versus temperature (tanδ-T) curves of the poled BNKT-FN system at various frequencies. ε_r at room temperature (RT) was found to increase with increasing FN amount. Permittivity at RT and frequency of 1 kHz were found for all samples and given as 1160 for $x=0$, 1485 for $x=0.01$, 1637 for $x=0.02$, 1933 for $x=0.03$ and 1760 for $x=0.04$. Permittivity maxima were found to decrease with the incorporation of FN and T_d was shifted to room temperature as the doping amount was increased.

According to recent reports, T_d is the thermal evolution of polar nanoregions (PNRs) and can result in a material transformation from ferroelectric to relaxor.[28] From the figure, it can be seen that the absence of prominent T_d in the current system at higher ratios could predict that the T_d peak is near to RT, which reveals that the relaxor behavior of these compounds increased with increasing FN.[28]

On the other hand, maximum permittivity temperature (T_m) remained nearly unchanged with FN doping ratio. In addition, enhancing of FN content steadily widened the anomaly at T_m signifying that BNKT-FN ceramics display the characteristic of diffusing phase transition, and hence, increased with the addition of FN content. The obtained permittivity behavior was in good agreement with those observed by Pham and Patterson et al. in the BNKT-based ceramics.[29,30]

Below 250°C, dielectric loss was found to be very small of values on the order of 0.01 and remained the same for all FN ratios with minor dispersion. However, at temperatures above 250°C, the dielectric loss was enhanced to values on the order of 0.036, which can be ascribed to thermally stimulated conductivity, particularly prominent at small frequencies (1 and 10 kHz).[11,31] This phenomenon can be described as the space charges in Bi-based systems with those having *A*-site deficiency creating charge vacancies because the

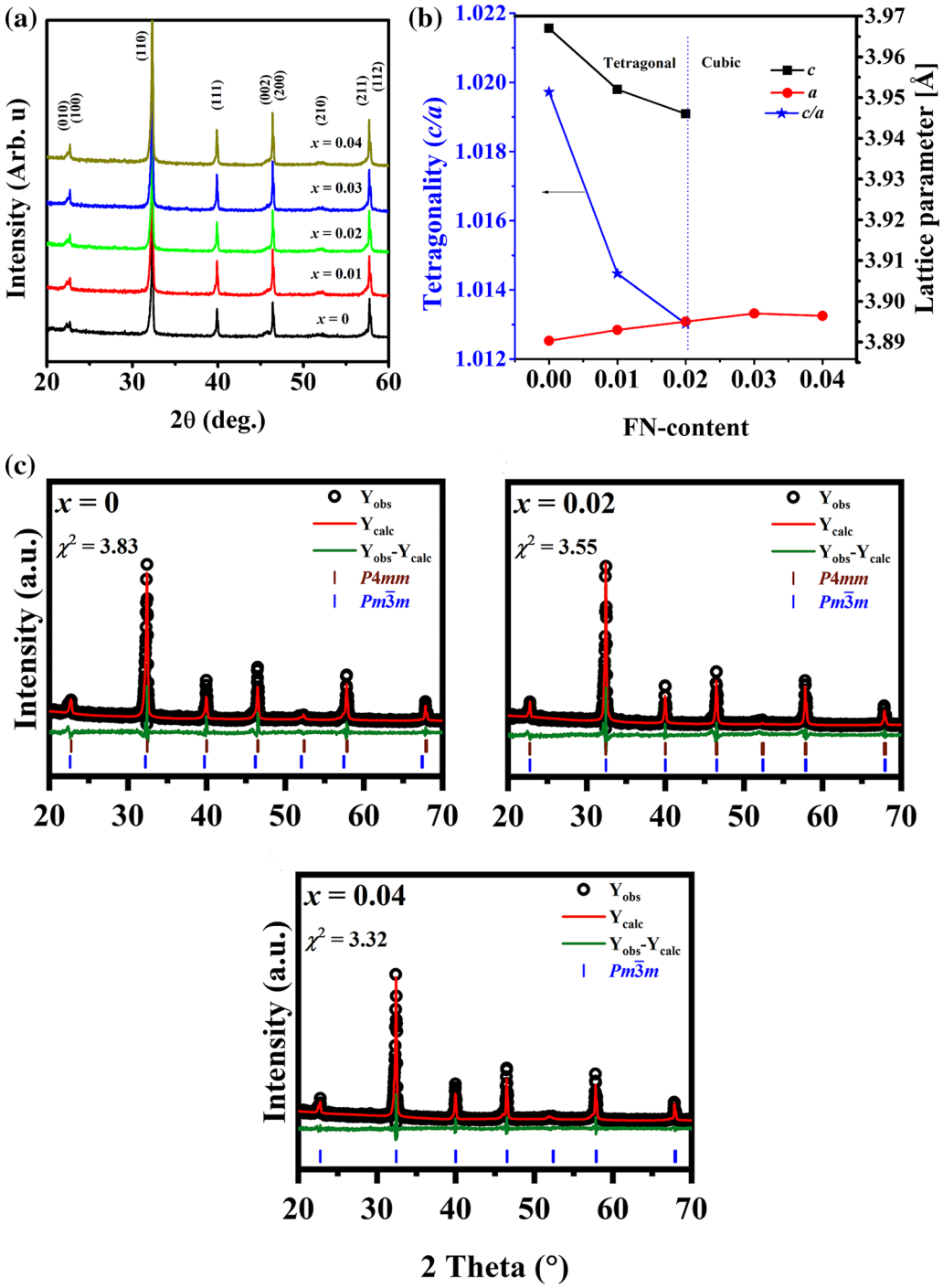

Fig. 1 (a) XRD plots of the BNKT-FN (x = 0, 0.01, 0.02. 0.03 and 0.04) system and (b) variation of lattice parameters and tetragonality with FN content and (c) Rietveld refinement of samples x = 0, 0.02 and 0.04.

evaporation of cations at the *A*-site at large sintering temperatures may cause an increase of loss.[6,8] From the discussions, it can be noted that the BNKT-FN system, which has a normal ferroelectric state (NF), is gradually transformed to a non-polar or relaxor phase when the FN ratio reached $x = 0.02$.

The diffusivity parameter of all samples was calculated in order to analyze the relaxation in the dielectric constant. Figure 4 presents the relationship between $\log(1/\varepsilon - 1/\varepsilon_m)$ and $\log(T - T_m)$ which gives diffusivity or degree of disorder (γ) at 1 kHz for the BNKT-FN ceramics.

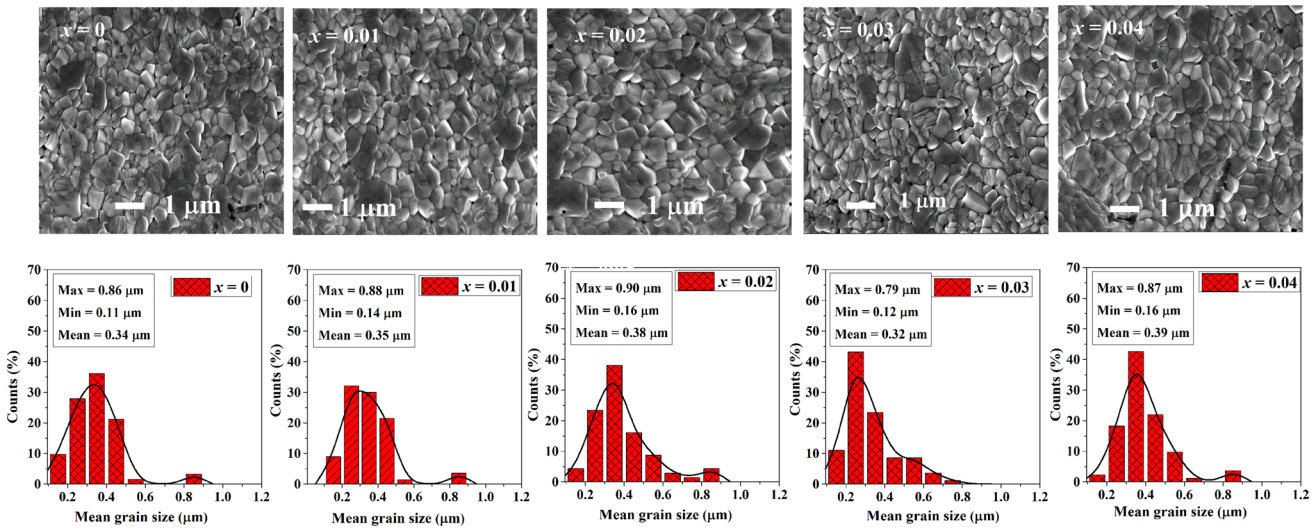

Fig. 2 Microstructural micrographs of the BNKT-FN system, with x = 0, 0.01, 0.02, 0.03 and 0.04.

Table I Physical and electrical properties of BNKT-FN ceramics sintered at 1150°C

BNKT-FN	Grain size (μm)	γ	ε_{max}	T_m (°C)	ε	d_{33} (pC/N)	P_r (μC/cm^2)	P_{max} (μC/cm^2)	E_c (kV/cm)	d^*_{33} (pm/V)
0	0.34	1.58	6461	291	1160	120	29.2	42.2	21.1	254
0.01		1.75	5388	296	1485	130	32.0	49.3	16.4	363
0.02	0.38	1.71	5129	298	1637	50	17.1	40.0	14.2	654
0.03	0.32	1.61	4989	301	1933	25	10.0	39.08	13.3	435
0.04	0.39	1.65	4538	301	1760	16	6.2	20.0	10.0	309

d^*_{33} is for normalized or dynamic strain

The formula $\log(1/\varepsilon - 1/\varepsilon_m) = \log K + \gamma \log(T - T_m)$ is used to describe the nature of diffusivity (γ).[32] The maximum dielectric constant (ε_m) in the formula will be the highest value of dielectric permittivity at T_m, while K is a constant. γ is a material constant that depends on the dopant amount and structure of the compound. For $\gamma = 1$, the ceramic can be described to be normal ferroelectric while the ceramics will be said to be a model relaxor ferroelectric for $\gamma = 2$.[33,34]

As shown in Fig. 4, the observed γ values are 1.58, 1.75, 1.71, 1.65 and 1.67 for $x = 0$, 0.01, 0.02, 0.03 and 0.04, respectively, representing a clear deviation by using the Curie–Weiss law for which $\gamma = 1$. The behavior confirms the manifestation of disarranging of dipoles in the investigated compound BNKT-FN.[35] Hence, the normal ferroelectric which has a long-range translational pattern was found to be interrupted by symmetry-breaking chemical disorder, and resulted in dielectric relaxation.[36,37]

According to the findings of this study, the observed relaxor behavior may be related to Bi, Na, and K occupying the *A*-sites in pure and (FeNb)/Ti ions at the *B*-sites of the BNKT-FN system.

Ferroelectric Response

Figure 5a exhibits polarization electric field (*P*-*E*) loops of the BNKT-FN piezoelectric compound. The detailed summary of the ferroelectric properties of the BNKT-FN system, such as remnant polarization (P_r) at $E = 0$ kV, coercive field (E_c) and maximum polarization (P_{max}) at 70 kV/cm are presented in Fig. 5b. For the undoped composition, the ferroelectric hysteresis loop has P_r 29.2 μC/cm^2, maximum polarization P_{max} of 42.2 μC/cm^2 and coercive field (E_c) of 21.1 kV/cm were observed. However, P_r first increased for $x = 0.01$ and then decreased for $x > 0.01$ while E_c was found to be decreased with the doping of FN concentration. The variation of the ferroelectric parameters is listed in Table I. The decrease in P_r with increasing FN content might be correlated to the growth of polar nano-regions induced by compositional disorder at the expense of long-range polar order.[6] Therefore, the undoped BNKT-FN system which has a normal ferroelectric state (NF) is now gradually transformed to a non-polar or relaxor phase when the FN ratio reached $x = 0.02$.

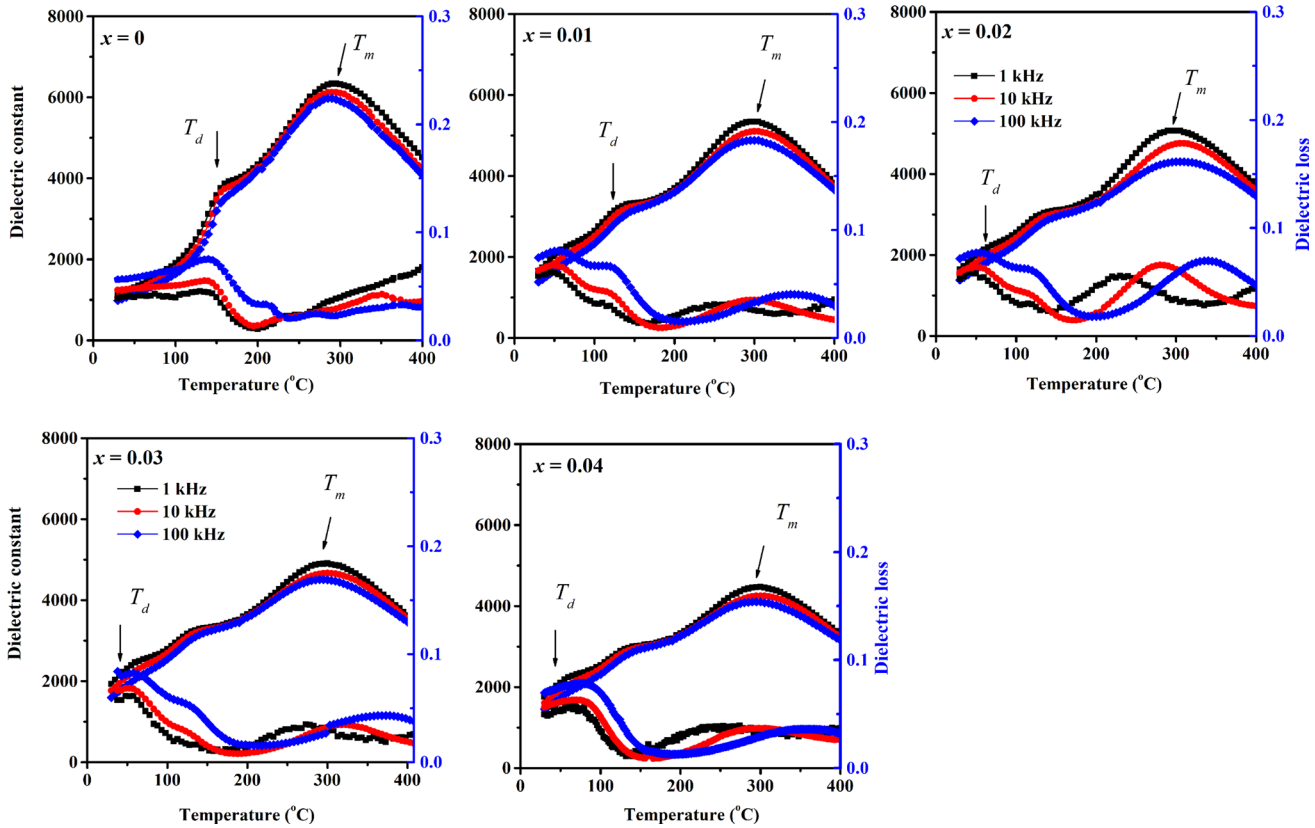

Fig. 3 Dielectric constant of the BNKT-FN (x = 0, 0.01, 0.02, 0.03 and 0.04) system at selected frequencies of 1, 10 and 100 kHz.

These characteristics demonstrate that the addition of FN content with an applied electric field disrupted long-range ferroelectric order, resulting in a relaxor or non-polar phase.[6,8,11] However, with the increasing amount of FN concentration to $x = 0.02$, the relaxor phase dominated, and the conversion from relaxor to ferroelectric level seems rather difficult due to drastic reduction in the maximum polarization of BNKT-FN piezoelectric ceramics.

Electromechanical Response

Figure 6 displays the bipolar electric field-induced strain plots of the piezoelectric BNKT-FN ceramics. The ferroelectric to relaxor transformation with increasing FN amount from undoped to critically doped composition can be well explained by bipolar strain. The unmodified sample, i.e. BNKT, exhibited a typical butterfly curve which has a negative strain value $\left(S_{neg} = 0.05\%\right)$ and is increased to $\left(S_{neg} = 0.13\%\right)$ for the sample $x = 0.01$ which can be related to the switching in the backward direction of domains, which again shows ferroelectricity in the sample.[32–37] A big decrease in the negative strain to $\left(S_{neg} = 0.02\%\right)$ and a simultaneous increase in the positive strain $(S = 0.36\%)$ for $x = 0.02$ was observed. EFIS study was clearly in agreement with that observed in the polarization study (Fig. 5). The increased value of the bipolar strain can be attributed to the co-occurrence of two phases, i.e. ergodic and nonergodic.[36,37] It was suggested that ergodicity is reversible and can be simply transformed to a ferroelectric state when an electric field is applied.[32–39] With a further increase in FN ratios, the value of strain dropped drastically and showed a paraelectric nature. The decrease in strain value suggests that the conversion from an ergodic phase to a ferroelectric phase is hard because the sample composition (3 mol.% FN) is far away from the state zone where two phases coexist.[40–42]

Figure 7 displays field-induced unipolar strain curves of BNKT-FN ceramics with $x = 0$–0.04 at an applied electric field of 55 kV/cm. It was observed that the strain improved significantly with enhancing FN amount up to critical composition, i.e. $x = 0.02$, but then decreased when the FN ratio was further increased. Undoped BNKT-FN ceramics exhibited a strain value of 0.16%. The strain level increased steadily up to 0.20% for 1 mol.% FN content; however, abruptly increased to 0.36% for the FN amount of 2 mol.% and then dropped with further increasing of FN content. Normalized strain S_{max}/E_{max} calculated from the ratio of the maximum strain $\left(S_{max}\right)$ to the maximum electric field $\left(E_{max}\right)$ for all BNKT-FN compositions are summarized in Fig. 7b. The

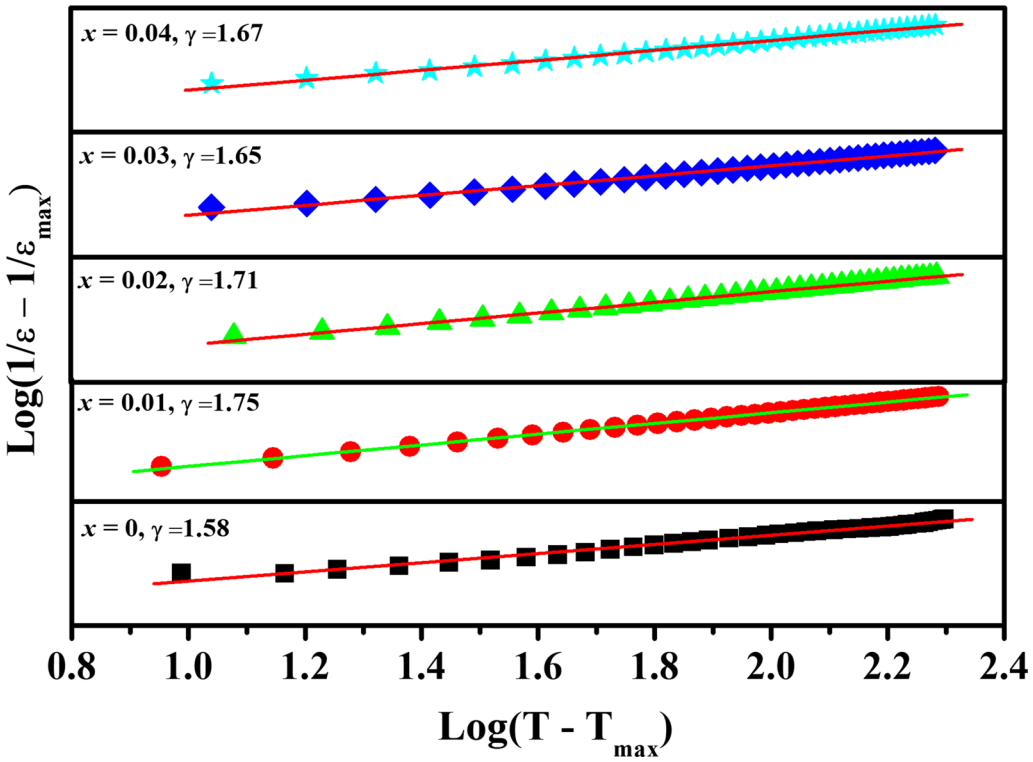

Fig. 4 Plots of the diffusivity (γ) at 1 kHz for the BNKT-FN ceramics.

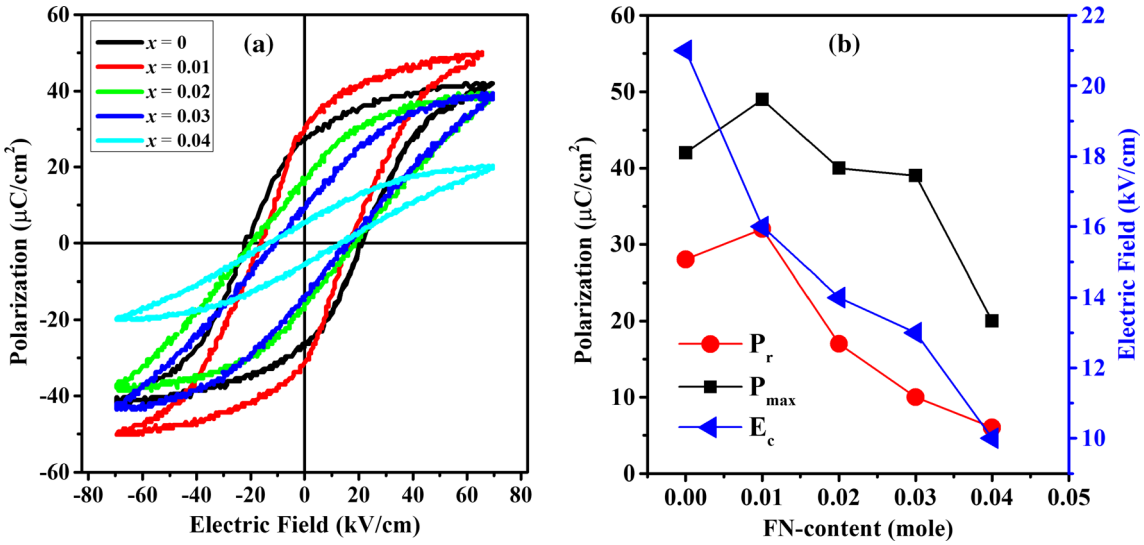

Fig. 5 (a) Polarization (P-E) loops and (b) ferroelectric properties (P_r, P_m, and E_c) of BNKT-FN ceramics.

observed normalized strain for unmodified BNKT-FN ceramic was 266 pm/V, which increased to 654 pm/V for 2 mol.% FN-modified BNKT-FN ceramics. The observed normalized strain value is significantly higher than that previously reported for BNT-based ceramics.[6,7] The comparison of the current strain value with the strain values of other BNKT-based[6,43–50] ceramics is shown in Table II. In sample $x=0$, strain produced under an electric field is not recoverable and may be attributed to rhombohedral lattice distortion. These findings show that high strain with the incorporation of FN ($x=0.02$) is a consequence of a reversible phase transition between a 'nonpolar' phase at zero field

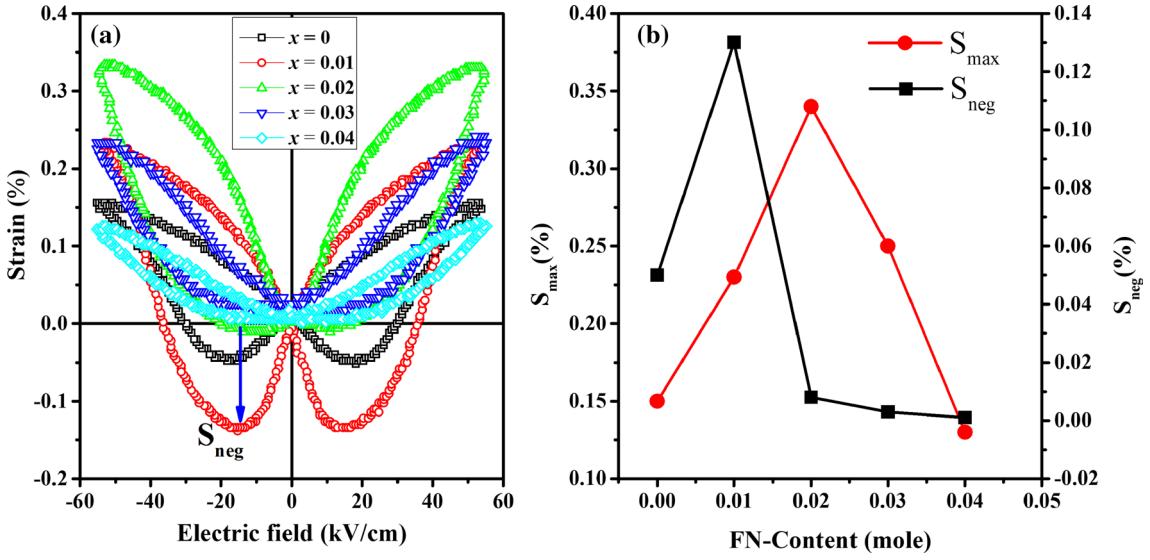

Fig. 6 (a) Bipolar strain loops and (b) variation of S_{max} and S_{neg} with FN content.

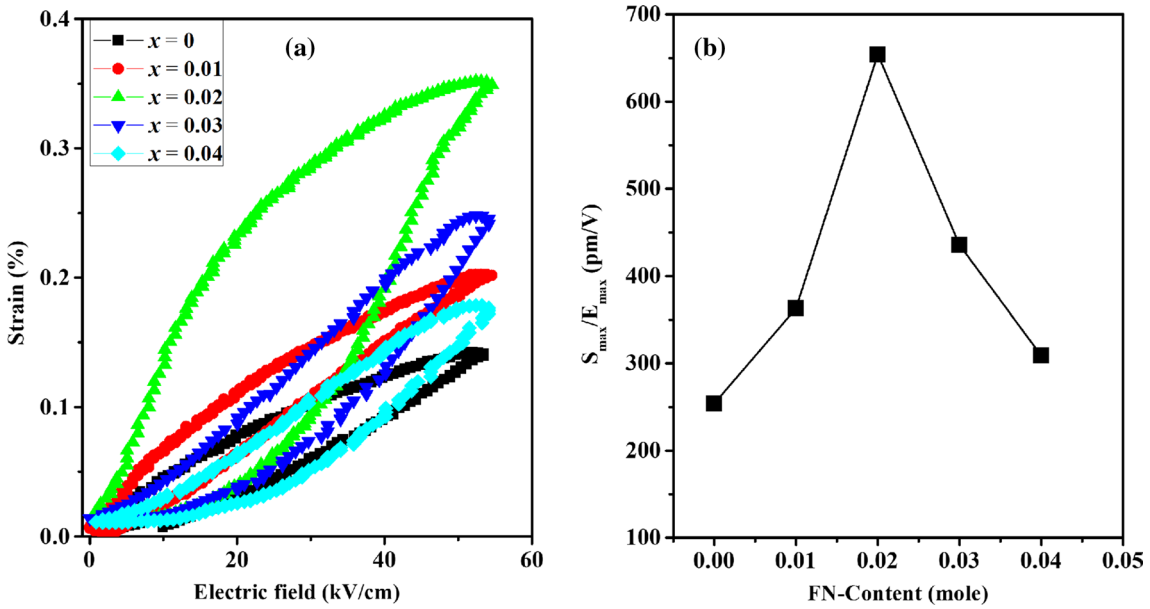

Fig. 7 (a) Unipolar strain and (b) variation of normalized strain as a function of FN content.

and a field-induced ferroelectric phase. Another reason may be due to the combined effects of the intrinsically high poling strain and the presence of a nonpolar phase which can be easily transformed to a ferroelectric state when an electric field is applied because of its comparable free energy as explained in the reports.[51,52] The partial substitution of the higher ionic size of combined Fe^{3+} (0.645 Å), and Nb^{5+} (0.60 Å) to the smaller ionic size of Ti^{4+} (0.605 Å) at the *B*–site. These characteristics describe that partial replacement of the complex-ion $(Fe_{1/2}Nb_{1/2})^{4+}$ for Ti^{4+} caused a local disruption in the crystal lattice as found in most of the Bi-based perovskites.[42,53,54] This distortion resulted in a ferroelectric to nonpolar phase transition in the system. For $x > 0.02$, the strain is dropped due to its paraelectric state, where polarization is almost non-existent.

Figure 8 displays the relationship of d_{33} with FN content. d_{33} was found to increase when the doping amount was 0.01 and then decreased for further doping of FN. The highest value was noted to be 132 pC/N. As static d_{33} is related to both dielectric constant (ε) and spontaneous polarization (P_s), so the degree of polarization can affect the static d_{33}.[55] Improvements in d_{33} for the $x = 0.01$ ceramics can also be attributed to the

Table II The comparison of dynamic strain values of other BNKT-based ceramics with the strain of current work

Year	Ceramics system	S_{max} (%)	E_{max} (kV/mm)	S_{max}/E_{max} (pm/V)	Reference
2021	BNKT-FN	0.36	5.5	654	Current
2014	$BNKTNb_x$-BST, $x=0.02$	0.38	6	634	6
2014	BNKT-BST-La_x, $x=0.02$	0.39	6	650	43
2014	$Bi_{1/2}(Na_{0.80}K_{0.20})_{1/2}TiO_3$-0.05Ba($Ti_{0.90}$ $Sn_{0.10}$)O_3	0.36	5.5	649	44
2012	$Bi_{0.5}(Na_{0.78}K_{0.22})_{1/2}(Ti_{1-x}Zr_x)O_3$, $x=0.03$	0.43	7	614	45
2012	$Bi_{1/2}(Na_{0.78}K_{0.22})_{1/2}TiO_3$-0.01($Bi_{1/2}La_{1/2}$)$AlO_3$	0.40	7	579	46
2015	$0.96[\{Bi_{1/2}Na_{0.84}K_{0.16})\}_{1-x-y}Li_xMg_y(Ti_{1-z}Nb_z)$ $O_3]$–$0.04SrTiO_3$	0.28	5	560	47
2011	$0.975[Bi_{1/2}(Na_{1-x}K_x)_{1/2}TiO_3]$–$0.025BiAlO_3$, $x=0.22$	0.33	6	533	48
2016	$(1-x)(Bi_{1/2}Na_{1/2}TiO_3$–$Bi_{1/2}K_{1/2}TiO_3$–$BaTiO_3)$–$xCaZrO_3$	0.35	7	500	49
2013	BNKT-CZ	0.37	6	603	50

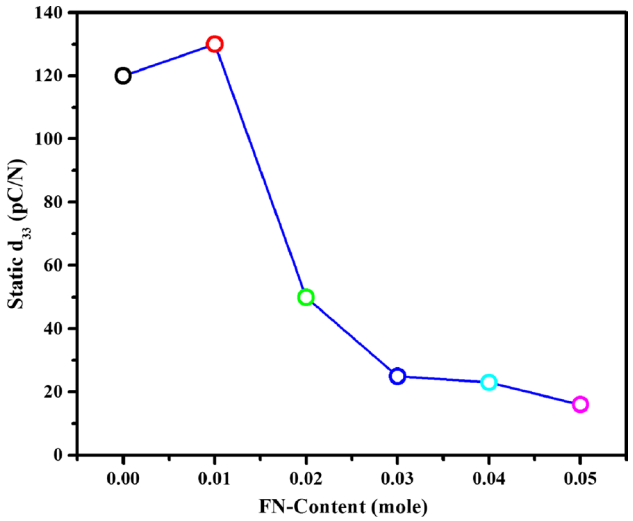

Fig. 8 Change in piezoelectric constant (static d_{33}) with FN content.

low coercive field E_c, which makes the poling more efficient. Therefore, the high d_{33} is attributed to the maximum P_r, P_s and the relatively low E_c of the sample $x=0.01$. For further doping, these ferroelectric parameters weakened and so d_{33} is dropped.

The observed high d_{33} can thus be attributed to the large $P_r$and ε of the BNKT-FN compound.

Figure 9a shows the variation of energy storage density and energy loss with FN content.

Using the following equations, we obtained the energy density for BNKT-FN system from the field dependent polarization.[56]

$$W_{total} = \int_0^{P_{max}} E\mathrm{d}P \tag{1}$$

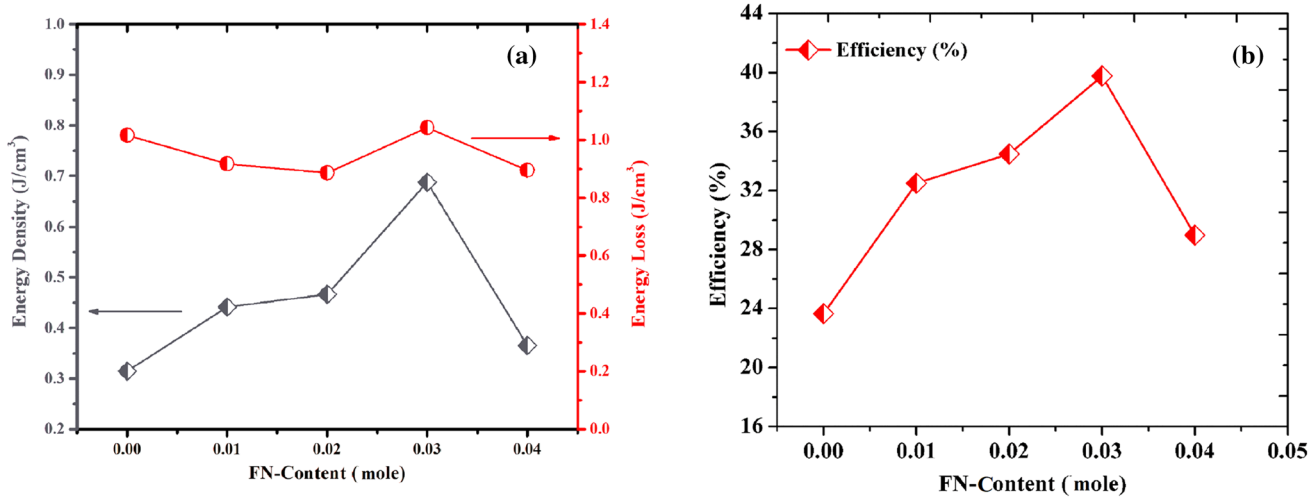

Fig. 9 (a) Variation of energy density with FN content, (b) Variation of efficiency with FN content.

$$W_{est} = \int_{P_r}^{P_{max}} E\mathrm{dP} \quad (2)$$

$$\eta = \frac{W_{est}}{W_{total}} \quad (3)$$

where W_{total} is the energy density and also energy loss and W_{est} is the energy storage density, while showing the energy storage efficiency (η). Figure 9a shows the variation of W_{total}, $W_{est,}$ and η with FN ratio at 60 kV/cm. Figure 9b displays the change in loss with respect to FN content at an applied field of 60 kV/cm.

With the increasing of FN content, the energy storage density increases at first and then dropped for further doping. The optimal energy density was found around 0.68 J/cm^3 at FN ratio 0.03. The monotonical improvement of energy density due to the slim *P-E* loops with high P_{max}-P_r value and energy density decreased with further decrease of P_{max}.[56,57] The energy loss was also found to vary with FN content doping. The loss was also monotonically decreased with FN content and then increased with additional FN doping.

Similarly, the energy storage efficiency (η) exhibited a gradual enhancement with increasing FN content. The highest η of 42% was obtained at $x = 0.03$, which may be due to the slim *P-E* loop with the lowest P_r and E_c. Sample with $x = 0.03$ is the optimal sample for the energy storage density.

Conclusions

In summary, piezoelectric ceramics $Bi_{1/2}(Na_{0.78}K_{0.22})_{1/2}Ti_{1-x}(Fe_{1/2}Nb_{1/2})_xO_3$ (BNKT-FN) with $x = 0$, 0.01, 0.02, 0.03, 0.04, were fabricated by CSSR. The FN content increase gradually broadened the dielectric anomaly at (T_m), suggesting that FN content induced a transition from a ferroelectric state to a nonpolar phase. P_r and E_c were found to decrease with increasing FN concentration which resulted in pinched hysteresis loops. A high normalized strain ($d_{33}^* = S_{max}/E_{max} = 654$ pm/V) was obtained at 2 mol.% of FN content. The optimal energy density was found around 0.68 J/cm^3 at FN ratio 0.03. The high energy storage efficiency η of 42% was obtained at $x = 0.03$, which may be due to the slim *P-E* loop with the lowest P_r and E_c. The $x = 0.03$ is the optimal sample for the energy storage density. Based on the results of the investigation, this system appears to be a promisi,ng environmentally friendly candidate for piezoelectric and energy-storage applications.

Acknowledgments This research was supported by the Basic Science Research Program through the National Research Foundation of Korea (NRF) funded by the Ministry of Education (NRF2021R1I1A1A01057086). F. Akram and A. Karoui are supported by DOE Award # NA0003979 and by NSAM-ML consortium, and by the DOE-CINT User Grant UNPUA No. 1344-07 2021.

Funding National Research Foundation of Korea, NRF-2021R1I1A1A01057086, Chang Won Ahn, NSAM-ML consortium, NA0003979, Fazli Akram.

Data Availability Research data are not shared.

Conflict of Interest The authors declare that they have no known competing financial interests or personal relationships that could have appeared to influence the work reported in this paper.

References

1. Y. Li, K.S. Moon, and C.P. Wong, Electronics Without Lead. *Science* 308, 1419 (2005).
2. T. Yamamoto, Ferroelectric Properties of the $PbZrO_3$-$PbTiO_3$ System. *Jpn. J. Appl. Phys.* 35, 5104 (1966).
3. L.E. Cross, Lead-Free at Last. *Nature* 432, 24 (2004).
4. G.A. Smolenskii, V.A. Isupov, A.I. Agranovskaya, and N.N. Krainik, New Ferroelectrics of Complex Composition. *Sov. Phys. Solid State* 2, 2651 (1961).
5. K.N. Pham, H.B. Lee, H.S. Han, J.K. King, J.S. Lee, A. Ullah, C.W. Ahn, and I.W. Kim, Dielectric, Ferroelectric, and Piezoelectric Properties of Nb- Substituted $Bi_{1/2}(Na_{0.82}K_{0.18})_{1/2}TiO_3$ Lead-Free Ceramics. *J. Kor. Phys. Soc.* 20, 60 (2012).
6. A. Ullah, R.A. Malik, A. Ullah, D.S. Lee, S.J. Jeong, J.S. Lee, I.W. Kim, and C.W. Ahn, Electric Field Induced Phase Transition and Large Strain in Lead-Free Nb-Doped BNKT-BST Ceramics. *J. Eur. Ceram. Soc.* 34, 29 (2014).
7. A. Sasaki, T. Chiba, Y. Mamiya, and E. Otsuki, Dielectric and Piezoelectric Properties of $(Bi_{0.5}Na_{0.5})TiO_3$-$(Bi_{0.5}K_{0.5})TiO_3$ System. *Jpn. J. Appl. Phy.* 38, 5564 (1999).
8. K. Yoshii, Y. Hiruma, H. Nagata, and T. Takenaka, Electrical Properties and Depolarization Temperature of $(Bi_{0.5}Na_{0.5})TiO_3$-$(Bi_{0.5}K_{0.5})TiO_3$ Lead-free Piezoelectric Ceramics. *Jpn. J. Appl. Phy.* 45, 4493 (2006).
9. P. Du, L. Luo, W. Li, Y. Zhang, and H. Chen, Photoluminescence and Electrical Performance Of Smart Material: Pr-Doped $(1-x)(Na_{0.5}Bi_{0.5})TiO_3$–$xCaTiO_3$ Ceramics. *J. Alloys Compd.* 551, 219 (2013).
10. A. Zeb and S.J. Milne, Stability in High Temperature Dielectric Properties for (1-x)$Ba_{0.8}Ca_{0.2}TiO_3$-x$Bi(Mg_{0.5}Ti_{0.5})_3$ Ceramics. *J. Am. Ceram. Soc.* 96, 2887 (2013).
11. K.N. Pham, A. Hussain, C.W. Ahn, I.W. Kim, S.J. Jeong, and J.S. Lee, Giant Strain in Nb- doped $Bi_{0.5}(Na_{0.82}K_{0.18})$ $0.5TiO_3$ Lead-Free Electromechanical Ceramics. *Mater. Lett.* 64, 2219 (2010).
12. T.H. Dinh, H.Y. Lee, C.H. Yoon, R.A. Malik, Y.M. Kong, and J.S. Lee, Effect of Lanthanum Doping on the Structural, Ferroelectric, and Strain Properties of $Bi_{1/2}(Na_{0.82}K_{0.18})_{1/2}TiO_3$ Lead-Free Ceramics. *J. Kor. Phys. Soc.* 62, 1004 (2013).
13. L.D. Vuong and P.D. Gio, Enhancement in Dielectric, Ferroelectric, and Piezoelectric Properties of $BaTiO_3$-Modified $Bi_{0.5}(Na_{0.4}K_{0.1})TiO_3$ Lead-Free Ceramics. *J. Alloy. Compd.* 817, 152790 (2020).
14. N.B. Do, H.-B. Lee, C.H. Yoon, J.K. Kang, and J.S. Lee, Effect of Ta-Substitution on the Ferroelectric and Piezoelectric Properties of $Bi_{0.5}$ $(Na_{0.82}K_{0.18})_{0.5}TiO_3$ Ceramics. *Trans. Electr. Electron. Mater.* 12, 64 (2011).
15. F. Akram, R.A. Malik, S. Lee, T.K. Song, and M.H. Kim, Thermally-Stable High Dielectric Properties of (1–*x*)

($0.65Bi_{1.05}FeO_3$–$0.35BaTiO_3$)–$x$$BiGaO_3$ Piezoceramics. *J. Eur. Ceram. Soc.* 39, 2304 (2019).

16. C.H. Hong, H.P. Kim, B.Y. Choi, H.S. Han, J.S. Son, C.W. Ahn, and W. Jo, Lead-Free Piezoceramics—Where to Move on? *J. Materiomics* 2, 1 (2016).
17. Y. Lei, Y. Chen, and J.D. Lee, Atomistic Study of Lattice Structure of $BiScO_3$. *Comput. Mater. Sci.* 41, 242 (2017).
18. F. Li, R. Zuo, D. Zheng, L. Li, and D. Viehland, Phase-Composition-Dependent Piezoelectric and Electromechanical Strain Properties in $(Bi_{1/2}Na_{1/2})TiO_3$-$Ba(Ni_{1/2}Nb_{1/2})O_3$ Lead-Free Ceramics. *J. Am. Ceram. Soc.* 98, 811 (2015).
19. D.E. Jain Ruth, S.M. Abdul Kader, M. Muneeswaran, N.V. Giridharan, D. Pathinettam Padiyan, and B. Sundarakannan, Structural and Electrical Properties of $(1-x)(Na_{0.5}Bi_{0.5})TiO_3$–$xBi(Mg_{0.5}Zr_{0.5})O_3$ Lead-Free Piezoelectric Ceramics. *Ceram. Int.* 42, 3330 (2016).
20. J. Huang, F. Zhu, D. Huang, B. Wang, T. Xu, X. Li, P. Fan, F. Xia, J. Xiao, and H. Zhang, Intermediate-Temperature Conductivity of B-Site Doped $Na_{0.5}Bi_{0.5}TiO_3$- Based Lead-Free Ferroelectric Ceramics. *Ceram. Int.* 42, 16798 (2016).
21. T.H. Dinh, J.K. Kang, J.S. Lee, N.H. Khansur, J. Daniels, H.Y. Lee, F.Z. Yao, K. Wang, J.F. Li, H.S. Han, and W. Jo, Nanoscale Ferroelectric/Relaxor Composites: Origin of Large Strain in lead–free Bi–Based Incipient Piezoelectric Ceramics. *J. Eur. Ceram. Soc.* 36, 3401 (2016).
22. L. Jin, F. Li, S. Zhang, and D.J. Green, Decoding the Fingerprint of Ferroelectric Loops: Comprehension of the Material Properties and Structures. *J. Am. Ceram. Soc.* 97, 1 (2014).
23. R. Peña-Garcia, A. Delgado, Y. Guerra, B.V.M. Farias, D. Martinez, E. Skovroinski, A. Galembeck, and E.P. Hernández, *Phys. Status Solidi A* 213, 2485 (2016).
24. X. Liu, B.H. Liu, F. Li, P. Li, J.W. Zhai, and B. Shen, Relaxor Phase Evolution and Temperature Insensitive Large Strain in B-Site Complex Ions Modified NBT-based Lead-Free Ceramics. *J. Mater. Sci.* 53, 309 (2018).
25. L. Li, J. Hao, Z. Xu, W. Li, and R. Chu, 0.46% Unipolar Strain in Lead-Free BNT-BT System Modified with Al and Sb. *Mater. Lett.* 184, 152 (2016).
26. R. Cheng, Z. Xu, R. Chu, J. Hao, J. Du, and G. Li, Electric Field-Induced Ultrahigh Strain and Large Piezoelectric Effect in $Bi_{1/2}Na_{1/2}TiO_3$-based Lead-Free Piezoceramics. *J. Eur. Ceram. Soc.* 36, 489 (2016).
27. H. Zang, J. Zhou, J. Shen, X. Yang, C. Wu, K. Han, Z. Zhao, and W. Chen, Enhanced Piezoelectric Property and Promoted Depolarization Temperature in Fe Doped $Bi_{1/2}(Na_{0.8}K_{0.2})_{1/2}TiO_3$ Lead-Free Ceramic. *Ceram. Int.* 43, 16395 (2017).
28. P. Fan, Y. Zhang, B. Xie, Y. Zhu, W. Ma, C. Wang, B. Yang, J. Xu, J. Xiao, and H. Zhang, Large Electric-Field-Induced Strain in B-Site Complex-Ion $(Fe_{0.5}Nb_{0.5})^{4+}$- Doped $Bi_{1/2}(Na_{0.82}K_{0.18})_{1/2}TiO_3$ Lead-Free Piezoceramics. *Ceram. Inter.* 44, 3211 (2018).
29. M. Ullah, H.U. Khan, A. Ullah, A. Ullah, I.W. Kim, I. Qazi, and I. Ahmad, Dielectric, Ferroelectric and Piezoelectric Properties of (1-x) $(Bi_{0.5}Na_{0.5})_{0.935}Ba_{0.065}Ti$ -x($LiSbO_3$) Solid Solutions. *Ceram. Inter.* 44, 556 (2018).
30. E.A. Patterson, D.P. Cann, J. Pokorny, and I.M. Reaney, Electromechanical Strain in Bi $(Zn_{1/2}Ti_{1/2})O_3$–$(Bi_{1/2}Na_{1/2})TiO_3$–$(Bi_{1/2}K_{1/2})TiO_3$ Solid Solutions. *J. Appl. Phys.* 111, 094105 (2012).
31. G.A. Smolenskii, V.A. Isupov, A.I. Agranovskaya, and N.N. Krainik, New Ferroelectrics of Complex Composition. *Sov. Phys. Solid State.* 2, 2651 (1961).
32. S.M. Pilgrim, A.E. Sutherland, and S.R. Winzer, Diffuseness as a Useful Parameter for Relaxor Ceramics. *J. Am. Ceram. Soc.* 73, 3122 (1990).
33. F. Akram, M. Habib, J. Bae, S.A. Khan, S.Y. Choi, T. Ahmed, S.B. Baek, S.T. Din, D.H. Lim, S.J. Jong, Y.S. Sung, T.K. Song, M.H. Kim, and S. Lee, Effect of Heat-Treatment Mechanism on Structural and Electromechanical Properties of Eco-Friendly (Bi, Ba)(Fe, Ti)O_3 Piezoceramics. *J. Mater. Sci.* 56, 13198 (2021).
34. K. Uchino and S. Nomura, Critical Exponents of the Dielectric Constants in Diffused-Phase-Transition Crystals. *Ferroelectrics* 44, 55 (1982).
35. Z. Yao, H. Liu, and L.C. Cao, Morphtropic Phase Boundary and Piezoelectric Properties of $(Bi_{1/2}Na_{1/2})_{1-x}$-$x(Bi_{1/2}K_{1/2})_xTiO_3$-$0.03(Na_{0.5}K_{0.5})NbO_3$ Ferroelectric Ceramics. *Mater. Lett.* 63, 547 (2009).
36. S.S.N. Bharadwaja, J.R. Kim, H. Ogihara, L.E. Cross, S.T. McKinstry, and C.A. Randall, Critical Slowing Down Mechanism and Reentrant Dipole Glass Phenomena in (1-x)$BaTiO_3$- $xBiScO_3$ ($0.1 \leq x \geq 0.4$): The High Energy Density Dielectrics. *Phy. Rev. B* 83, 024106 (2011).
37. V. Bovtun, S. Veljko, S. Kamba, J. Petzelt, S. Vakhrushev, Y. Yakymenko, K. Brinkman, and N. Setter, Broad-Band Dielectric Response of $PbMg_{1/3}Nb_{2/3}O_3$ relaxor Ferroelectrics: Single Crystals, Ceramics and Thin Films. *J. Eur. Ceram. Soc.* 286, 7 (2006).
38. J. Hao, W. Bai, and W. Li, Phase Transitions, Relaxor Behavior, and Large Strain Response in LiNbO3-Modified $Bi_{0.5}(Na_{0.80}K_{0.20})_{0.5}TiO_3$ Lead-Free Piezoceramics. *J. Appl. Phys.* 114, 044103 (2013).
39. W. Bai, P. Li, L. Li, J. Zhang, B. Shen, and J. Zhai, Structure Evolution and Large Strain Response in BNT–BT Lead-Free Piezoceramics Modified with $Bi(Ni_{0.5}Ti_{0.5})O_3$. *J. All. Compd.* 649, 772 (2015).
40. W. Bai, L. Li, W. Li, B. Shen, J. Zhai, and H. Chen, Phase Diagrams and Electromechanical Strains in Lead-Free BNT-based Ternary Perovskite Compounds. *J. Am. Ceram. Soc.* 97, 3510 (2014).
41. P. Jaita, A. Watcharapasorn, and S. Jiansirisomboon, Investigation of a New Lead-Free $Bi_{0.5}(Na_{0.40}K_{0.10})$ TiO_3-$(Ba_{0.7}Sr_{0.3})$ TiO_3 Piezoelectric Ceramics. *Non. R. Lett.* 7, 24 (2012).
42. S.Y. Cheng, J. Shieh, H.Y. Lu, C.Y. Shen, Y.C. Tang, and N.J. Ho, Structure Analysis of Bismuth Sodium Titanate-based A-site Relaxor Ferroelectrics by Electron Diffraction. *J. Eur. Ceram. Soc.* 33, 2141 (2013).
43. A. Ullah, A. Ullah, I.W. Kim, D.S. Lee, S.J. Jeong, and C.W. Ahn, Large Electromechanical Response in Lead-Free La-Doped BNKT–BST Piezoelectric Ceramics. *J. Am. Ceram. Soc.* 97, 2471 (2014).
44. P. Jaita, A. Watcharapasorn, D.P. Cann, and S. Jiansirisomboon, Dielectric, Ferroelectric and Electric Field-Induced Strain Behavior of $Ba(Ti_{0.90}Sn_{0.10})O_3$-Modified $Bi_{0.5}(Na_{0.80}K_{0.20})_{0.5}TiO_3$ Lead -Free Piezoelectrics. *J. Alloys Compd.* 596, 98 (2014).
45. A. Hussain, C.W. Ahn, J.S. Lee, A. Ullah, and I.W. Kim, Large Electric-Field-Induced Strain in Zr-Modified Lead- Free $Bi_{0.5}(Na_{0.78}K_{0.22})_{0.5}TiO_3$ Piezoelectric Ceramics. *Sens. Actuators A* 158, 84 (2010).
46. A. Ullah, C.W. Ahn, S.Y. Lee, J.S. Kim, and I.W. Kim, Structure, Ferroelectric Properties, and Electric Field-Induced Large Strain in Lead-Free $Bi_{0.5}(Na,K)_{0.5}TiO_3$-$(Bi_{0.5}La_{0.5})AlO_3$ Piezoelectric Ceramics. *Ceram. Int.* 38S, S363 (2012).
47. R.A. Malik, A. Hussain, A. Zaman, A. Maqbool, J.U. Rahman, T.K. Song, W.J. Kim, and M.H. Kim, Structure–Property Relationship in Lead-Free A- and B-Site Co-Doped $Bi_{0.5}(Na_{0.84}K_{0.16})_{0.5}TiO_3$–$SrTiO_3$ Incipient Piezoceramic. *RSC Adv.* 5, 96953 (2015).
48. A. Ullah, C.W. Ahn, A. Hussain, S.Y. Lee, J.S. Kim, and I.W. Kim, Effect of Potassium Concentration on the Structure and Electrical Properties of Lead-Free $Bi_{0.5}$ $(Na,K)_{0.5}$ TiO_3-$BiAlO_3$ Piezoelectric Ceramics. *J Alloy compd.* 509, 3148 (2011).

49. L. Wu, S. Zhang, J. Liu, Q. Hu, J. Chen, Y. Wang, B. Xu, Y. Xia, J. Yin, and Z. Liu, The Electrical Properties of (1-x)($Bi_{0.5}Na_{0.5}TiO_3$–$Bi_{0.5}K_{0.5}$ TiO_3–$BaTiO_3$)–x$CaZrO_3$ Lead-Free Piezoelectric Ceramics. *Ceram. Int.* 42, 13783 (2016).
50. H.B. Lee, D.J. Heo, R.A. Malik, C.H. Yoon, H.S. Han, and J.S. Lee, Lead-Free $Bi_{1.2}(Na_{0.82}K_{0.18})_{1/2}TiO_3$ Ceramics Exhibiting Large Strain with Small Hysteresis. *Ceram. Int.* 39, S705 (2013).
51. W. Jo, T. Granzow, E. Aulbach, J. Rödel, and D. Damjanovic, Origin of the Large Strain Response in $(K_{0.5}Na_{0.5})NbO_3$-Modified $(Bi_{0.5}Na_{0.5})TiO_3$-$BaTiO_3$ Lead-free Piezoceramics. *J. Appl. Phys.* 105, 094102 (2009).
52. A. Ullah, C.W. Ahn, A. Hussain, S.Y. Lee, and I.W. Kim, Phase Transition, Electrical Properties, and Temperature-Insensitive Large Strain in $BiAlO_3$-Modified $Bi_{0.5}(Na_{0.75}K_{0.25})_{0.5}TiO_3$ Lead-Free Piezoelectric Ceramics. *J. Am. Ceram. Soc.* 94, 3915 (2011).
53. Y. Hiruma, H. Nagata, and T. Takenaka, Detection of Morphotropic Phase Boundary of$(Bi_{0.5}Na_{0.5})TiO_3$–$Ba(Al_{0.5}Sb_{0.5})O_3$ Solid-Solution Ceramics. *Appl. Phys. Lett.* 95, 052903 (2009).
54. J. Fu, R. Zuo, S.C. Wu, J.Z. Jiang, L. Li, T.Y. Yang, X. Wang, and L. Li, Electric Field Induced Intermediate Phase and Polarization Rotation Path in Alkaline Niobate Based Piezoceramics Close to the Rhombohedral and Tetragonal Phase Boundary. *Appl. Phys. Lett.* 100, 122902 (2012).
55. D. Damjanovic, Ferroelectric, Dielectric and Piezoelectric Properties of Ferroelectric Thin Films and Ceramics. *Rep. Prog. Phys.* 61, 1267 (1998).
56. F. Weyland, H. Zhang, and N. Novak, Enhancement of Energy Storage Performance by Criticality in Lead-Free Relaxor Ferroelectrics. *Phys. Status. Solidi. R.* 12, 1800165 (2018).
57. S. Pang, L. Yang, J. Qin, H. Qin, H. Xie, H. Wang, C. Zhou, and J. Xu, Low Electric Field-Induced Strain and Large Improvement in Energy Density of $(Lu_{0.5}Nb_{0.5})^{4+}$ Complex-Ions Doped BNT–BT Ceramics. *App. Phy. A.* 125, 119 (2019).